

Article

# Selective Chlorination and Extraction of Valuable Metals from Iron Precipitation Residues

Lukas Höber \*, Kerrin Witt and Stefan Steinlechner \* 

Christian Doppler Laboratory for Selective Recovery of Minor Metals Using Innovative Process Concepts, Chair of Nonferrous Metallurgy, Montanuniversität Leoben, Franz Josef Strasse 18, 8700 Leoben, Austria; kerrin.witt@unileoben.ac.at

\* Correspondence: lukas.hoeber@unileoben.ac.at (L.H.); stefan.steinlechner@unileoben.ac.at (S.S.)

**Featured Application:** Authors are encouraged to provide a concise description of the specific application or a potential application of the work. This section is not mandatory.

**Abstract:** Due to the aggravating situations regarding climate change, resource supply, and land consumption by the landfilling of residual materials, it is necessary to develop recycling processes that allow the recovery of valuable metals from industrial residues with significantly reduced CO<sub>2</sub> emissions. In this context, it is conceivable that processes using chlorination reactions will be of importance in the future. The simultaneous selective chlorination and evaporation of nine valuable metals was evaluated theoretically and experimentally in small-scale STA trials; then, it was tested practically on six different iron precipitation residues from the zinc and nickel industries. The metal chlorides FeCl<sub>3</sub>·6H<sub>2</sub>O and MgCl<sub>2</sub>·6H<sub>2</sub>O were identified as the most effective reactants, resulting in high extraction rates for the metals In, Ag, Zn, Pb, Au, and Bi, while lower yields are achievable for Sn, Cu, and Ni. Iron, which is predominant in volume in the residual materials, shows lower chlorination tendencies which allows the effective separation of the valuable elements of interest from the iron containing matrix.

**Keywords:** selective chlorination; jarosite recycling; multimetal recovery; CO<sub>2</sub> reduction



**Citation:** Höber, L.; Witt, K.; Steinlechner, S. Selective Chlorination and Extraction of Valuable Metals from Iron Precipitation Residues. *Appl. Sci.* **2022**, *12*, 3590. <https://doi.org/10.3390/app12073590>

Academic Editors: Dibyendu Sarkar, Rupali Datta, Prafulla Kumar Sahoo and Mohammad Mahmudur Rahman

Received: 9 March 2022

Accepted: 30 March 2022

Published: 1 April 2022

**Publisher's Note:** MDPI stays neutral with regard to jurisdictional claims in published maps and institutional affiliations.



**Copyright:** © 2022 by the authors. Licensee MDPI, Basel, Switzerland. This article is an open access article distributed under the terms and conditions of the Creative Commons Attribution (CC BY) license (<https://creativecommons.org/licenses/by/4.0/>).

## 1. Introduction

Among humanity's greatest challenges for the next generations is the shift to CO<sub>2</sub>-free processes for energy generation, transportation, and the production of basic materials and goods for the globalized society. A key role in this context is assigned to industry, since many processes depend on the use of carbon not only as an energy source but also as a chemical reactant. Another critical aspect of heavy industry is the continued landfilling of various residual materials. For Europe, the resource issue is essential, as the continent is already dependent on exports for many technology materials. In the long term, the global and especially the European markets are facing the absolute necessity of developing recycling processes for the recovery of valuable metals which emit significantly less greenhouse gas emissions during the process. A category of waste materials that are predominantly immobilized and disposed without recovery of the contained valuable metals are iron-containing precipitation residues such as jarosite and goethite, which are generated in the course of the hydrometallurgical production of zinc and nickel. Jarosite precipitation is by far the most important method for iron removal. The formed precipitates have the mineralogical structure XFe<sub>3</sub>(SO<sub>4</sub>)<sub>2</sub>(OH)<sub>6</sub> with X being represented by monovalent cations such as Na<sup>+</sup>, K<sup>+</sup>, NH<sub>4</sub><sup>+</sup>, and H<sub>3</sub>O<sup>+</sup> or valuable elements such as Ag<sup>+</sup> or 1/2Pb<sup>2+</sup> [1–3]. Goethite describes an iron hydroxide with the formula FeO·OH [3]. In the precipitated products of the zinc industry, significant amounts of zinc and lead can be found as well as lower concentrations of indium, silver, copper, and other valuable elements [4–7]. Jarosites

from the nickel industry contain nickel [8] and arsenic. Over the past decades, a variety of methods have been developed for the processing of iron precipitation residues [9]. The only globally used process is the immobilization of jarosite in the so-called Jarofix process, in which the material is chemically stabilized by the addition of Portland cement, lime, and water and subsequently landfilled. Approaches were investigated where jarosite is mixed with clay, fly ash, and water [10,11] or marble processing rejects [12] to produce brick materials for building purposes. Other research stated the possibility of producing materials for road or dump construction by mixing jarosite with ferrous slags [13,14]. Furthermore, the residue can substitute sand in concrete mixtures [15]. Jarosite from the nickel industry was successfully tested as an alternative substitute for gypsum in cement mixtures [16]. For goethite, a concept was introduced whereby the material is mixed with blast furnace and converter slag, leading to the formation of a hard rock-like material [17]. The majority of research projects for the recovery of valuable elements or conversion of the residue into products were carried out in the field of hydrometallurgical treatment methods. The bioleaching of jarosite residues bears the potential of recovering valuable elements with low energy and chemicals consumption [18–20]. Furthermore, the materials can be converted into magnetite or hematite, which for example can be used theoretically in the pigment or iron and steel industry [21–23]. Alkaline leaching and the subsequent cyanidation of precious metals, especially silver [5,24–27], the combined treatment of sewage sludge and jarosite [28], leaching with  $\text{NH}_4\text{Cl}$  to recover Pb, Cu, Cd, and Ag [6], roasting and flotation to recover silver and anglesite [29], as well as the usage of resins [30] can also be considered as relevant developments on a laboratory scale. The use of deep-eutectic solvents for the recovery of zinc was investigated to treat goethite [31]. The residual materials can also be treated in pyrometallurgical processes, whereby it was stated that a small number of zinc-producing companies use common technologies such as TSL reactors or waelz kilns to co-treat jarosite or goethite with other residues [32]. Other approaches such as the treatment of zinc plant residues in plasma furnaces [33,34], the reduction and magnetic separation to recover zinc [35], as well as the production of glass-ceramics from goethite [36,37] can be named. However, there are no generally applied methods on an industrial scale—although some zinc plants were reported to process a part of their iron precipitation residues, they remain exceptions. The chlorination of valuable elements was as well proposed in the field of recycling precipitation residues, stating that indium can be extracted as indium chloride at temperatures over 800 °C [38]. This was subsequently confirmed in small-scale trials, where electric arc furnace dust as a chlorine carrier and coal were added to jarosite waste and treated at 1100 °C, leading to the extraction of silver, indium, and lead in noteworthy extents [39]. A similar approach focused on the simultaneous extraction of zinc, lead, copper, indium, and silver by mixing jarosite with coal and  $\text{CaCl}_2$  as a chlorine-bearing additive [40].

Generally, it can be summarized that processes in both categories bear significant disadvantages. Hydrometallurgical approaches are generally designed for the recovery of specific elements and often rely on narrow parameter ranges; the developed pyrometallurgical processes, on the other hand, are generally associated with the emission of greenhouse gases whereby the implementation becomes questionable in the future.

The novel recycling approach presented in this paper is based on the chlorination and extraction of valuable metals from the excess iron matrix of the precipitation residues without the addition of carbon as a reactant. The schematic process flow sheet is provided in Figure 1. The residues are mixed in their original or thermally treated (decomposed) form with suitable metal chlorides and processed at moderate temperatures of up to 1100 °C. The underlying principle of the extraction is the fact that the metal chlorides evaporate at significantly lower temperatures compared to their metallic or oxidic form. Iron shows lower thermodynamic tendencies to chloride formation than the valuable metal compounds contained in precipitation residues. Process control without carbon addition results in significantly lower specific greenhouse gas emissions. Furthermore, the formation

of problematic chlorine–carbon compounds is prevented. In addition, the treatment at low temperatures does not result in the formation of liquid phases.

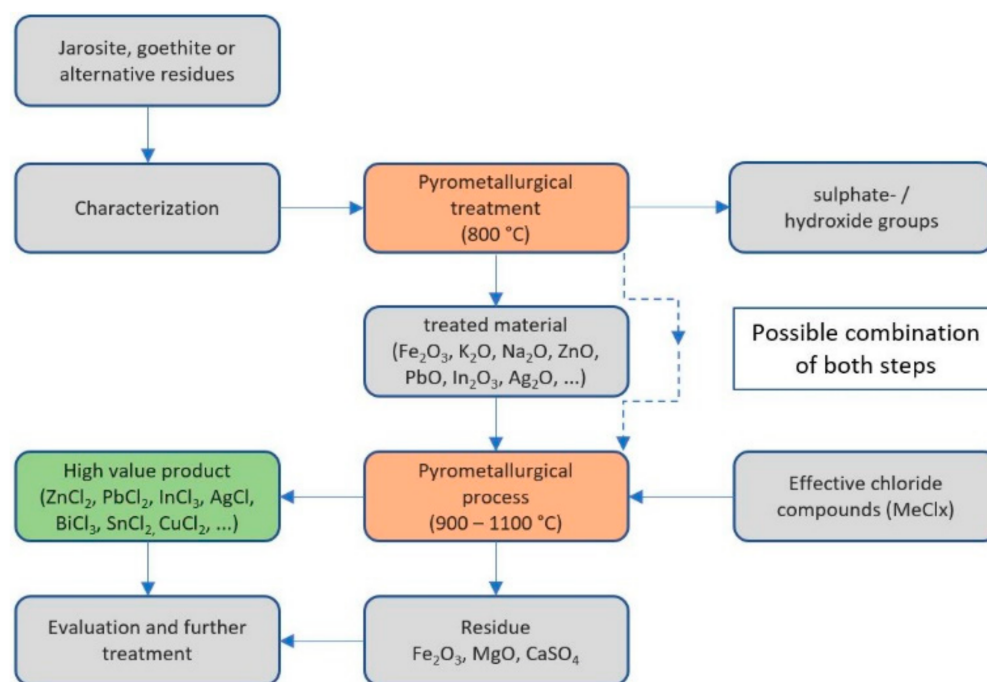


**Figure 1.** Concept flow sheet of the chlorination process for treating precipitation residues.

## 2. Theoretical Considerations and Thermodynamic Calculations

The potential of recovering valuable metals from residual materials by means of chlorination has been demonstrated repeatedly. Indium can be recovered from spent LCDs using polyvinyl chloride (PVC) [41,42] or aqueous HCl [43]; furthermore, the contained metals in CIGS–solar cells (copper–indium–gallium–selenium) can be extracted to noteworthy extents using chlorine gas or ammonium chloride [44]. Li et al. proposed the possibility of recovering Au and Ag from cyanide tailings using CaCl<sub>2</sub> [45]. Pyrite (FeS<sub>2</sub>) addition positively influences the chlorination of Au as the formation of CaSO<sub>4</sub> results in the liberation of chlorine [46]. NH<sub>4</sub>Cl was stated to extract Zn via chlorination from steel mill dusts (BOS) [47]; a similar approach was developed for recovering Zn and also Pb from EAFD by treatment in an Ar–Cl<sub>2</sub> atmosphere. Comprehensive investigations were carried out in the field of chlorination of valuable elements from municipal solid waste (MSW) using HCl for Zn and Pb [48], PVC for Cu, Zn, Pb, and Cd [49]. Furthermore, metal chlorides such as NaCl, CaCl<sub>2</sub>, and MgCl<sub>2</sub> were investigated, leading to noteworthy extraction of Cd, Cr, Cu, Ni, Pb, or Zn [50,51].

In the course of this work, the reactivity of various solid metal chlorides for multimetal recovery from an excess iron matrix was investigated. Metal chlorides are present in huge extents worldwide and used in various applications. The six compounds NaCl, KCl, CaCl<sub>2</sub>, MgCl<sub>2</sub>, AlCl<sub>3</sub>, and FeCl<sub>3</sub> were investigated regarding their reactivity for chlorinating valuable elements from residual materials. It can be stated that the chlorination of a metal of interest is highly dependent on the present form of the element chlorine itself. Hereby, three different ways for supplying chlorine by metal chlorides can be cited, being the liberation of gaseous chlorine, the liberation of gaseous hydrochloric acid, and the direct reaction of the solid, liquid, or gaseous metal chloride compound.

For example, the chlorination of Zn from ZnO using gaseous HCl proceeds according to the following reaction:  $\text{ZnO} + 2\text{HCl}(\text{g}) \leftrightarrow \text{ZnCl}_2(\text{g}) + \text{H}_2\text{O}(\text{g})$ . The demand of chlorination agent depends on the valency of the respective valuable elements. It is noteworthy in this context that all mentioned chlorides except NaCl and KCl are strongly hygroscopic (Ropp, 2013; Wiberg et al., 2007) and therefore are generally present in a partially hydrated

form. Thermodynamic calculations which were carried out using the software packages FactSage (Bale et al., 2016) and HSC Chemistry V10 (Metso Outotec) revealed that NaCl and KCl are significantly more stable than the other compounds, showing no or very little tendency for reaction with valuable metal oxides.

Calculations using HSC chemistry V10 show that the chlorides  $\text{CaCl}_2$ ,  $\text{MgCl}_2$ ,  $\text{AlCl}_3$ , and  $\text{FeCl}_3$  in their hydrated form ( $\text{MeCl}_x \cdot n\text{H}_2\text{O}$ ) show a different behavior regarding their ability to liberate gaseous hydrochloric acid. For the theoretical interpretation of the equilibrium composition of chemical reactions in dependence of temperature, the Free Gibbs Energy (Delta-G) can be considered, whereby negative values indicate that the reaction proceeds in the given direction. For  $\text{CaCl}_2$  and  $\text{MgCl}_2$ , there are three different types of hydrates ( $n\text{H}_2\text{O}$  with  $n$  being 2, 4, or 6), while for the trivalent chlorides  $\text{AlCl}_3$  and  $\text{FeCl}_3$ , solely the hexahydrate compounds are available in the used database. The values for Delta-G in dependence of the temperature for both the solo or multiple-step dehydration (splitting of water leaving the pure metal chloride) and the hydrolysis (splitting of HCl and  $\text{H}_2\text{O}$  leading to the formation of the metal oxide) are given in Figure 2. When assuming an actual trial mixture to heat up to processing temperature, the depicted data suggest that for the three chlorides  $\text{MgCl}_2 \cdot 6\text{H}_2\text{O}$ ,  $\text{FeCl}_3 \cdot 6\text{H}_2\text{O}$ , and  $\text{AlCl}_3 \cdot 6\text{H}_2\text{O}$ , the chemical driving force is higher for liberating gaseous hydrochloric acid than for splitting of solely the water groups (values of dashed lines are more negative than the ones of solid lines). For  $\text{MgCl}_2 \cdot 6\text{H}_2\text{O}$ , this accounts for all three possible steps of dehydration or hydrolysis. This effect cannot be stated for  $\text{CaCl}_2 \cdot 6\text{H}_2\text{O}$ , where the values for liberating water are more negative at given temperatures, indicating that the compound is unlikely to set free the highly reactive gaseous hydrochloric acid.

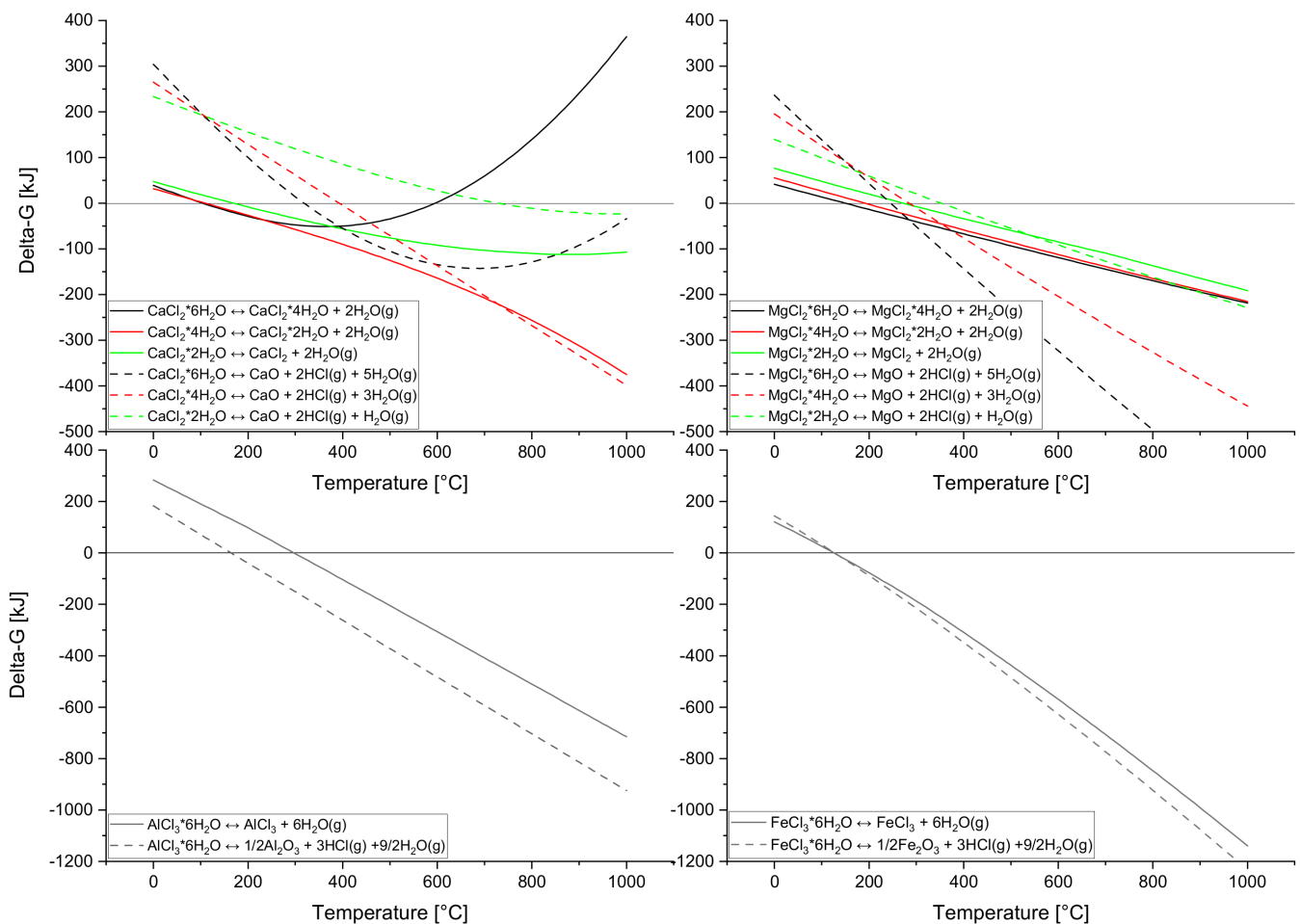


**Figure 2.** Calculated Delta-G values for hydrolysis or dehydration of the hydrated metal chlorides.

The main aspect concerning the recovery of valuable metals by selective chlorination and evaporation is the low evaporation temperature  $T_{\text{vap}}$  of the formed metal chlorides compared to the elements in metallic or oxide form. Figure 3a shows the values for  $T_{\text{vap}}$  of the elements of interest in various compound forms. Sulfate compounds are not included because they would generally react to oxides under the liberation of sulfur–oxygen compounds. All elements except silver evaporate completely as chlorides at temperatures below 1000 °C. In this context, it must be pointed out that all chlorides have significant vapor pressures even at lower temperatures, and extraction is effectively possible even for silver, as will be shown below. In addition to the individual values for  $T_{\text{vap}}$ , the range of the averaged values of all metals and oxides as well as those of the chlorides is shown. The difference between the evaporation temperatures of the compound types is significant, leading to the general conclusion that elements of value are effectively extractable in their chloridic form. Furthermore, the software package FactSage with the database FactPS was used to calculate the values for Delta-G for the reactions of the elements of interest as well as iron in the form of oxides with gaseous HCl under formation of the metal chlorides, as given in Figure 3b. Since the software considers the compounds in their most stable form at given temperatures, the slopes of the curves change due to melting and evaporation. The dashed red line shows the values of Delta-G for the reaction of  $\text{Fe}_2\text{O}_3$ . It can be stated that the curve is in the positive area for the majority of the temperature range. This is the theoretical basis for the selective multimetal separation from the iron matrix, which accounts for 30–40% (elemental Fe) in the iron precipitation residues, depending on the actual residue. The only other elements that show positive values are copper and nickel. The reaction of indium is in equilibrium at temperatures over 600 °C (Delta-G = 0).

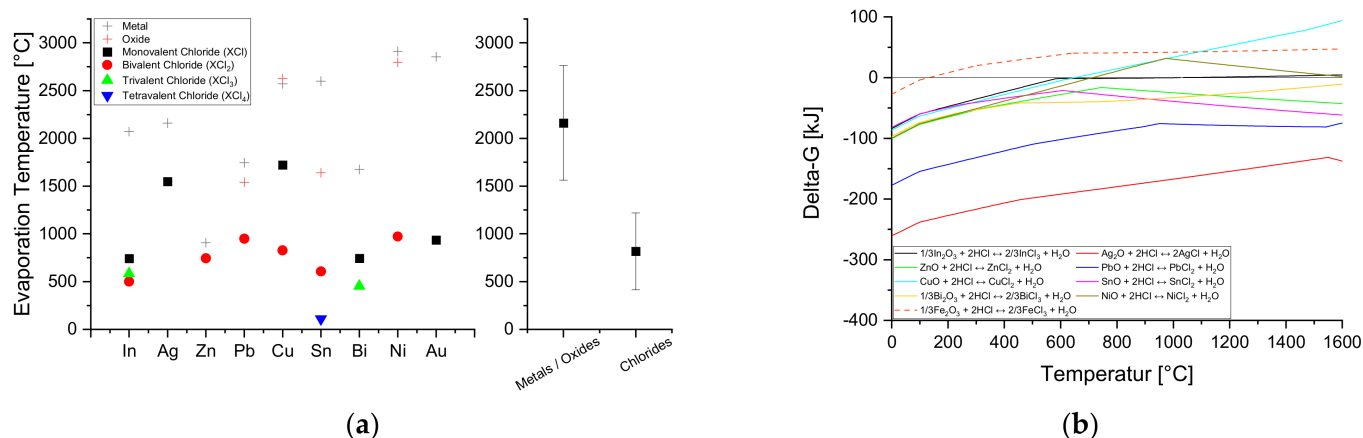


**Figure 3.** (a) Evaporation temperatures of the valuable metals in metallic, chloridic, and oxidic form; (b) Delta-G values for reactions of metal oxides with hydrochloric acid.

### 3. Materials and Methods

To confirm the reactivity of the assessed metal chlorides as well as the potential extraction of multiple valuable elements, two different experimental approaches were conducted. The behavior of all six metal chlorides  $\text{NaCl}$ ,  $\text{KCl}$ ,  $\text{CaCl}_2 \cdot 6\text{H}_2\text{O}$ ,  $\text{MgCl}_2 \cdot 6\text{H}_2\text{O}$ ,  $\text{AlCl}_3 \cdot 6\text{H}_2\text{O}$ , and  $\text{FeCl}_3 \cdot 6\text{H}_2\text{O}$  in their pure form was investigated, using simultaneous thermal analysis (STA). Furthermore, trials were carried out with mixtures of metal chlorides and valuable elements of interest in form of oxides and sulfates. For an evaluation of the concept with real residual materials, chlorination campaigns were executed in a muffle furnace with untreated as well as pre-treated iron precipitation residues (decomposed structure) in mixtures with specific metal chlorides, which were identified as effective.

#### 3.1. STA Campaigns with Pure Substances

As part of the fundamental research,  $\text{NaCl}$ ,  $\text{KCl}$ ,  $\text{CaCl}_2 \cdot 6\text{H}_2\text{O}$ ,  $\text{MgCl}_2 \cdot 6\text{H}_2\text{O}$ ,  $\text{AlCl}_3 \cdot 6\text{H}_2\text{O}$ , and  $\text{FeCl}_3 \cdot 6\text{H}_2\text{O}$  were analyzed using STA regarding their behavior for liberating chlorine

or hydrochloric acid. For the STA trials with mixtures, the metals silver, indium, lead, zinc, and nickel were investigated. The following oxides and sulfates in the form of pure chemicals were used for the preparation of the following mixtures:  $\text{Ag}_2\text{O}$ ,  $\text{Ag}_2\text{SO}_4$ ,  $\text{In}_2\text{O}_3$ ,  $\text{In}_2(\text{SO}_4)_3$ ,  $\text{NiO}$ ,  $\text{PbO}$ , and  $\text{ZnO}$ . Based on the thermodynamic calculations performed beforehand, the chlorides  $\text{AlCl}_3 \cdot 6\text{H}_2\text{O}$ ,  $\text{FeCl}_3 \cdot 6\text{H}_2\text{O}$ , and  $\text{MgCl}_2 \cdot 6\text{H}_2\text{O}$  were selected as chlorination agents, respectively, for each of the metal oxides and sulfates. Furthermore,  $\text{In}_2\text{O}_3$  was mixed with  $\text{NaCl}$ ,  $\text{KCl}$ , and  $\text{CaCl}_2 \cdot 6\text{H}_2\text{O}$  to confirm the significantly lower suitability of those chlorides (based on thermodynamic evaluations and the trials with pure chlorides). According to the chlorination reactions described in the thermodynamics section, the metal chlorides  $\text{AgCl}$ ,  $\text{InCl}_3$ ,  $\text{PbCl}_2$ ,  $\text{ZnCl}_2$ , and  $\text{NiCl}_2$  were expected to be formed during chlorination. In reference to the stoichiometry of the reactions, the mixtures were prepared using an excess molar amount of chlorine with a chlorination agent to metal oxide/sulfate ratio of 1.5. The STA was performed using a Netzsch 409PC analyzer with synthetic air ( $\text{N}_2/\text{O}_2 = 80/20$ ) as purge gas and a flow rate of 0.3 L/min. Sintered  $\text{Al}_2\text{O}_3$  crucibles and a sample mass of 100 mg were used; all chemicals were purchased in laboratory grade. All trials were carried out with a constant heating rate of 20 K/min from 20 °C to a maximum temperature of 1000 °C, 1200 °C, or 1400 °C. The assessment of the STA trials was conducted by evaluating the collected data (mass loss over time, temperature) and comparing the real mass of the solid residual materials in the crucible to the one expected based on theoretical calculations for each mixture.

### 3.2. Campaigns with Industrial Iron Precipitation Residues

Various iron precipitation residues were investigated and processed in defined mixtures in a muffle furnace (Nabertherm LT9/12) in a scale of 80 g. The main purposes for the trial campaign consisting of 108 experiments are at first the identification of the most effective chlorination agents for the extraction of specific metals as well as for the multi-metal recovery from various industrial residues with partly low concentrations of valuable elements. Furthermore, the influence of increasing the concentration of the respective chlorination agent as well as higher process temperatures are evaluated.

The raw materials in use were jarosite and goethite residues of the zinc industry as well as a jarosite residue originating in the nickel production. Each material was tested in its original form as well as thermally pre-treated (calcined) in a muffle furnace at 800 °C for five hours using air as atmosphere in order to decompose the mineral structures to simpler oxidic and sulfatic compounds. Chemical analyses were conducted for the untreated as well as for the pre-calcined materials at two accredited laboratories; the results are shown in Table 1.

The chlorides  $\text{AlCl}_3 \cdot 6\text{H}_2\text{O}$ ,  $\text{FeCl}_3 \cdot 6\text{H}_2\text{O}$ , and  $\text{MgCl}_2 \cdot 6\text{H}_2\text{O}$  were used as chlorination agents, which is premised on the thermodynamic calculations and STA trials.

The trial setup is the treatment of the mixture in an open crucible which is charged into the furnace, leading to the evaporation of a share of chloride without taking part in the targeted reactions. Furthermore, it has to be pointed out that chemical reactions do not occur ideally. Therefore, the trials were carried out with an excess of chlorine supply. The 2-fold of the total calculated stoichiometric chlorine demand for full chlorination of considered valuable elements and 5% of iron was set as the base chlorine addition. As it is of interest if the extraction of certain elements can be significantly increased by the higher addition of the respective chlorides, the experiments were carried out with 2-fold and 3-fold of the base value chlorine addition for all three chlorides.

It was assumed in the course of the calculations that the valuable element chlorides that are formed during the treatment of jarosite, goethite, calcined jarosite, and calcined goethite are  $\text{AgCl}$ ,  $\text{BiCl}_3$ ,  $\text{CuCl}_2$ ,  $\text{InCl}_3$ ,  $\text{KCl}$ ,  $\text{NaCl}$ ,  $\text{PbCl}_2$ ,  $\text{SnCl}_2$ , and  $\text{ZnCl}_2$ . The chlorination of iron in all trials was considered to an extent of 5%, forming the trivalent compound  $\text{FeCl}_3$ . For the trials with nickel jarosite (original and calcined), the chlorine demand was calculated for the full chlorination of nickel and in turn 5% of Fe. The elements Na and K are considered due to their partly high concentration in precipitation residues, which would lead to

significant chlorine consumption due to their affinity for chloride formation. In reference to these suppositions, the calculation of the mixture ratios for the trials was executed. Each jarosite and goethite material, untreated as well as pre-treated, was mixed with each of the mentioned chlorination agents in the three proposed mixing ratios. The resulting practically used mixtures are shown in Table S1 (Supplementary Materials). R represents the amount of residual material, and CA represents the mass of the respective chlorination agent. After the preparation of a mixture of milled dry residual material and chlorination agent, an amount of 80 g was filled into a silica crucible. The crucible was charged into a muffle furnace at trial temperature where the mass decrease was tracked via an integrated balance. Each mixture was tested at two different temperatures, 900 °C and 1100 °C, with air as atmosphere. After 30 min, the crucible was removed from the furnace to cool down at ambient air temperature, and the remaining solid residue was milled and analyzed. Test data considered are mass loss and chemical analysis of the final material.

**Table 1.** Chemical analysis of the investigated original and calcined iron precipitation residues.

Concentration [wt %]	Jarosite	Goethite	Ni-Jarosite	Jarosite Calcined	Goethite Calcined	Ni-Jarosite Calcined
Structural Elements						
Fe	25.6 ± 1.8	29.1 ± 1.9	36.6 ± 0.3	39.9 ± 1.7	36.6 ± 1.3	61.9 ± 2.3
S	13.83 ± 0.24	7.16 ± 0.33	6.38 ± 0.08	7.86 ± 0.04	6.61 ± 0.02	0.19 ± 0
K	2.77 ± 0.05	0.2 ± 0	0.08 ± 0.01	4.03 ± 0.05	0.23 ± 0.05	0.12 ± 0
Na	1.46 ± 0.06	<0.05	0.01 ± 0	2.24 ± 0.15	0.06 ± 0.01	0.15 ± 0.01
Ca	0.53 ± 0.02	4.78 ± 0.24	0.01 ± 0	0.78 ± 0.01	6.08 ± 0.03	0.01 ± 0
As	0.42 ± 0.01	0.19 ± 0.01	0.26 ± 0	0.63 ± 0.01	0.23 ± 0	0.45 ± 0.01
Mg	0.19 ± 0	0.15 ± 0	<0.01	0.30 ± 0	0.18 ± 0	<0.01
Al	0.37 ± 0	0.89 ± 0.03	0.19 ± 0.02	0.56 ± 0	1.10 ± 0	0.26 ± 0
Valuable Elements						
Zn	3.57 ± 0.07	9.60 ± 0.21	0	5.37 ± 0.05	11.90 ± 0.08	0
Pb	1.26 ± 0	0.68 ± 0	0.06 ± 0	1.9 ± 0	0.84 ± 0	0.08 ± 0
Ni			3.08 ± 0.04			5.43 ± 0.26
[ppm]						
In	591 ± 3	410 ± 9	0	882 ± 11	495 ± 9	0
Ag	282 ± 40	136 ± 32	0	403 ± 79	194 ± 26	0
Cu	2713 ± 25	9113 ± 67	47 ± 2	4053 ± 5	11,000	68 ± 2
Sn	1703 ± 26	308 ± 6	<20	2617 ± 52	376 ± 5	<20
Bi	941 ± 8	181 ± 2	17 ± 1	1440 ± 20	224 ± 3	28 ± 0
[ppb]						
Au	367 ± 9	264 ± 13	73 ± 10	547 ± 18	333 ± 103	114 ± 8

Considering the chemical analyses of the used iron precipitation residues in the mixture and the solid residues of each experiment, the calculation of extraction rates  $e_{EI}$  for the elements of interest in percent was performed according to Equation (1):

$$e_{EI} = \left( 1 - \frac{x_{EI(Fin)} * m_{Fin}}{x_{EI(Res)} * m_{Start} * f_R} \right) * 100\% \quad (1)$$

where  $m_{Start}$  is the mass of the mixture (g),  $f_R$  is the respective share of precipitation residue in the mixture, and  $m_{Fin}$  represents the mass of final solid residue from the chlorination treatment (g). Furthermore,  $x_{EI(Res)}$  represents the concentration of element EI in the iron precipitation residue (wt %), and  $x_{EI(Fin)}$  represents the concentration of element EI in the final solid residue (wt %).

Due to the high number of calculated extraction rates in trials with residues for the zinc industry and the resulting difficulty in evaluating the overall process performance,

an evaluation factor was calculated that summarizes the respective extraction rates as a function of the element concentration and the current market price of the metals. The factor (Equation (2)) is referred to as *valex* (value extraction) and enables the evaluation of the tests in monetary terms with regard to the simultaneous recovery of all considered valuable metals. The elements considered in calculating the *valex* values were In, Ag, Zn, Pb, Cu, Sn, Au, and Bi. The calculated *valex* factor ranges from 0 to 1 whereby it has to be stated that the amount of residue in the mixture is not considered, therefore giving only information of the extraction itself but not on the actual economic performance. The *valex* factor can be interpreted as the theoretic recovery of economic potential from the respective trial mixture.

$$\text{valex} = \frac{\sum x_{\text{El(Res)}} * P_{\text{El}} * e_{\text{El}}}{\sum x_{\text{El(Res)}} * P_{\text{El}}} \quad (2)$$

$P_{\text{El}}$  represents the following respective market prices as of December 2021 as given in Table 2.

**Table 2.** Market prices of the considered metals as of 29 December 2021.

Metal	Ag [52]	Au [53]	Bi [54]	Cu [55]	In [56]	Pb [57]	Sn [58]	Zn [59]
Price [€/kg]	640	50,900	6.41	8.5	390	2.04	35	3.16

## 4. Results

### 4.1. STA Trials

The objective of testing pure metal chlorides is to gather information on their potential as chlorine-liberating compounds. Figure 4a depicts the mass loss in the STA trials with NaCl and KCl showing full evaporation within the maximum temperature range. The whole amount of sample material was evaporated, indicating no release of chlorine. The highlighted peaks in the DTA signal show the melting points of the chlorides. The assumed behavior that  $\text{CaCl}_2 \cdot 6\text{H}_2\text{O}$  reacts to  $\text{CaCl}_2$  (no splitting of HCl) was confirmed according to Figure 4b. The theoretical remaining mass when reacting to  $\text{CaCl}_2$  was calculated (black horizontal line), which covers precisely with the experimental curve.  $\text{MgCl}_2 \cdot 6\text{H}_2\text{O}$  shows the opposite characteristic as the curve covers with the theoretical value for remaining MgO (evaporation of HCl). Both reactions appear to proceed stepwise. Figure 4c depicts the mass curve for the trial with  $\text{AlCl}_3 \cdot 6\text{H}_2\text{O}$ , which shows one continuous mass drop to the exact theoretic value of the remaining  $\text{Al}_2\text{O}_3$  (full liberation of HCl). For  $\text{FeCl}_3 \cdot 6\text{H}_2\text{O}$ , the mass decrease appears in steps, and the final experimentally determined mass is below the theoretical value, which could be attributed to the fact that HCl is not entirely liberated, leading to the partial evaporation of  $\text{FeCl}_3$  itself. This is in line with the theoretical evaluations illustrated in Figure 2, where the two curves of reactions with  $\text{FeCl}_3 \cdot 6\text{H}_2\text{O}$  (hydrolysis and dehydration) are almost identical at lower temperatures. The data in Figure 4d, which summarize the trial series with  $\text{In}_2\text{O}_3$  and all six chlorides, confirm that NaCl and KCl are not suitable for chlorination, as the remaining mass is very close to the calculated values for remaining  $\text{In}_2\text{O}_3$  (no chlorination reaction). In a mixture of  $\text{In}_2\text{O}_3$  and  $\text{CaCl}_2 \cdot 6\text{H}_2\text{O}$  (green line), a first mass decrease, which is associated with the splitting of water, is followed by a stable period up to 1100 °C and a subsequent mass decrease, which is not completed at the final temperature of 1400 °C. This can be attributed to a reaction of liquid  $\text{CaCl}_2$  with the present indium oxide followed by the evaporation of  $\text{InCl}_3$ . However, compared to the trials with  $\text{MgCl}_2 \cdot 6\text{H}_2\text{O}$ ,  $\text{AlCl}_3 \cdot 6\text{H}_2\text{O}$ , and  $\text{FeCl}_3 \cdot 6\text{H}_2\text{O}$ , the result is poor, as they show almost full chlorination and evaporation (first two mentioned) and a precisely covering curve for iron chloride.

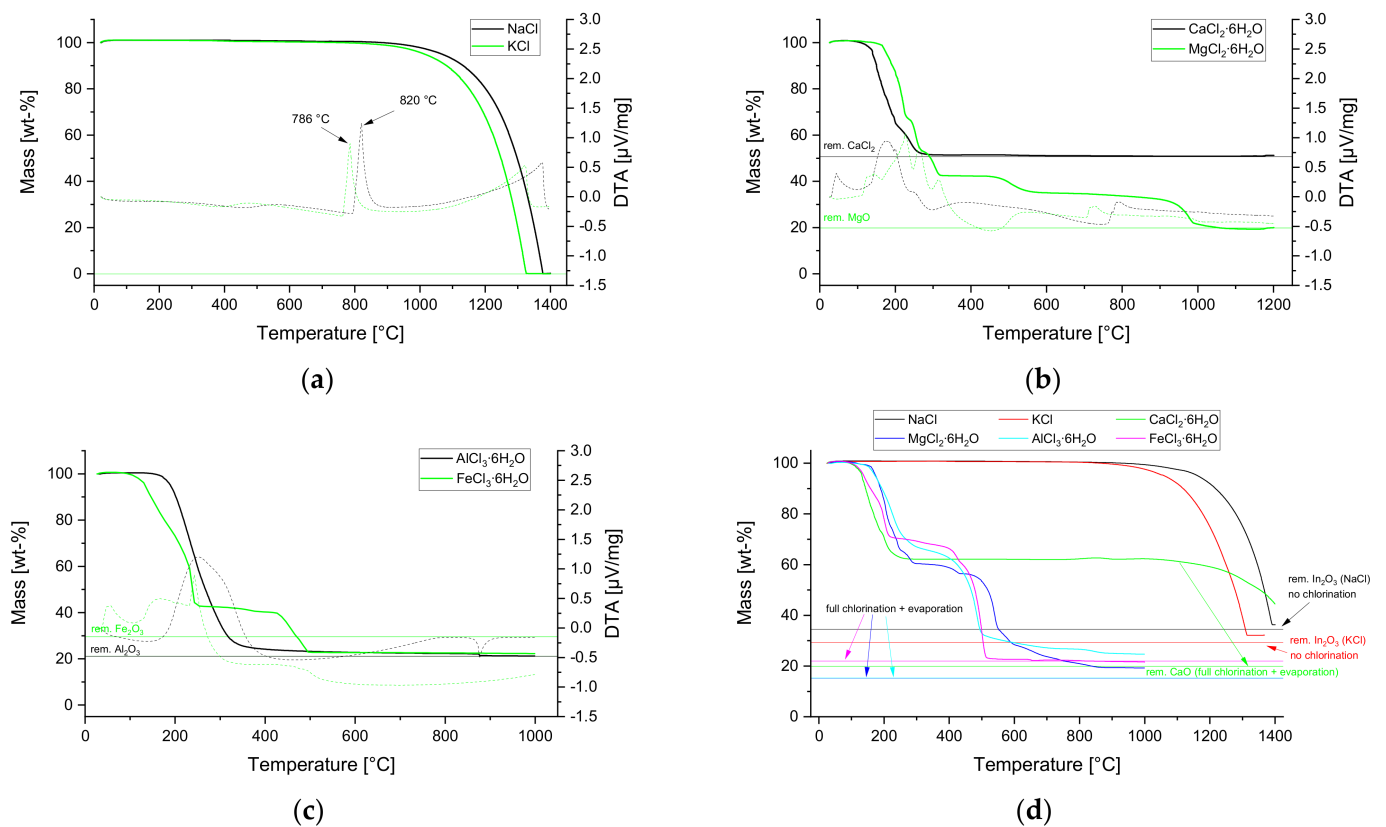


**Figure 4.** Results of STA experiments with (a) monovalent, (b) bivalent, and (c) trivalent metal chlorides; (d) comparison of thermogravimetric tests with indium oxide (1.5 times stoichiometric chlorine extent).

Figure 5a–f confirm the practical effectivity of the three utilized chlorides  $\text{MgCl}_2 \cdot 6\text{H}_2\text{O}$ ,  $\text{AlCl}_3 \cdot 6\text{H}_2\text{O}$ , and  $\text{FeCl}_3 \cdot 6\text{H}_2\text{O}$  as chlorination agents for further assessed valuable metal compounds. As depicted, silver chlorination (Figure 5a) proceeds effectively according to the fact that the curves cover with the theoretical remaining mass values for the chlorine carrier oxides. This is in order with the findings in Figure 3a where silver chlorination shows the highest thermodynamic driving force of all elements. As assumed, evaporation starts at elevated temperatures compared to the trials with  $\text{In}_2\text{O}_3$  (Figure 4d),  $\text{ZnO}$ , and  $\text{PbO}$  (Figure 5b,c). The chlorination of  $\text{NiO}$  works insufficiently with the actual mass loss being significantly lower than the theoretical calculated values (Figure 5d). In mixtures where indium is present as sulfate, as shown in Figure 5e, it is observed that chlorination seems to be hindered, as the experimental final mass is significantly higher than the calculated values. For silver sulfate (Figure 5f), the effect is not as pronounced but still detectable compared to trials with silver oxide. It is noteworthy that in both campaigns, the three curves show mass drops in the same order with rising temperature (Fe before Al before Mg), which can be attributed to the splitting of  $\text{SO}_3$  ( $\text{SO}_2 + 1/2\text{O}_2$ , respectively). This is in line with findings in the literature stating decomposition temperatures of 530 °C for  $\text{Fe}_2(\text{SO}_4)_3$  [60], 610 to 990 °C for  $\text{Al}_2(\text{SO}_4)_3$  [61], and 1085 °C for  $\text{MgSO}_4$  [62].

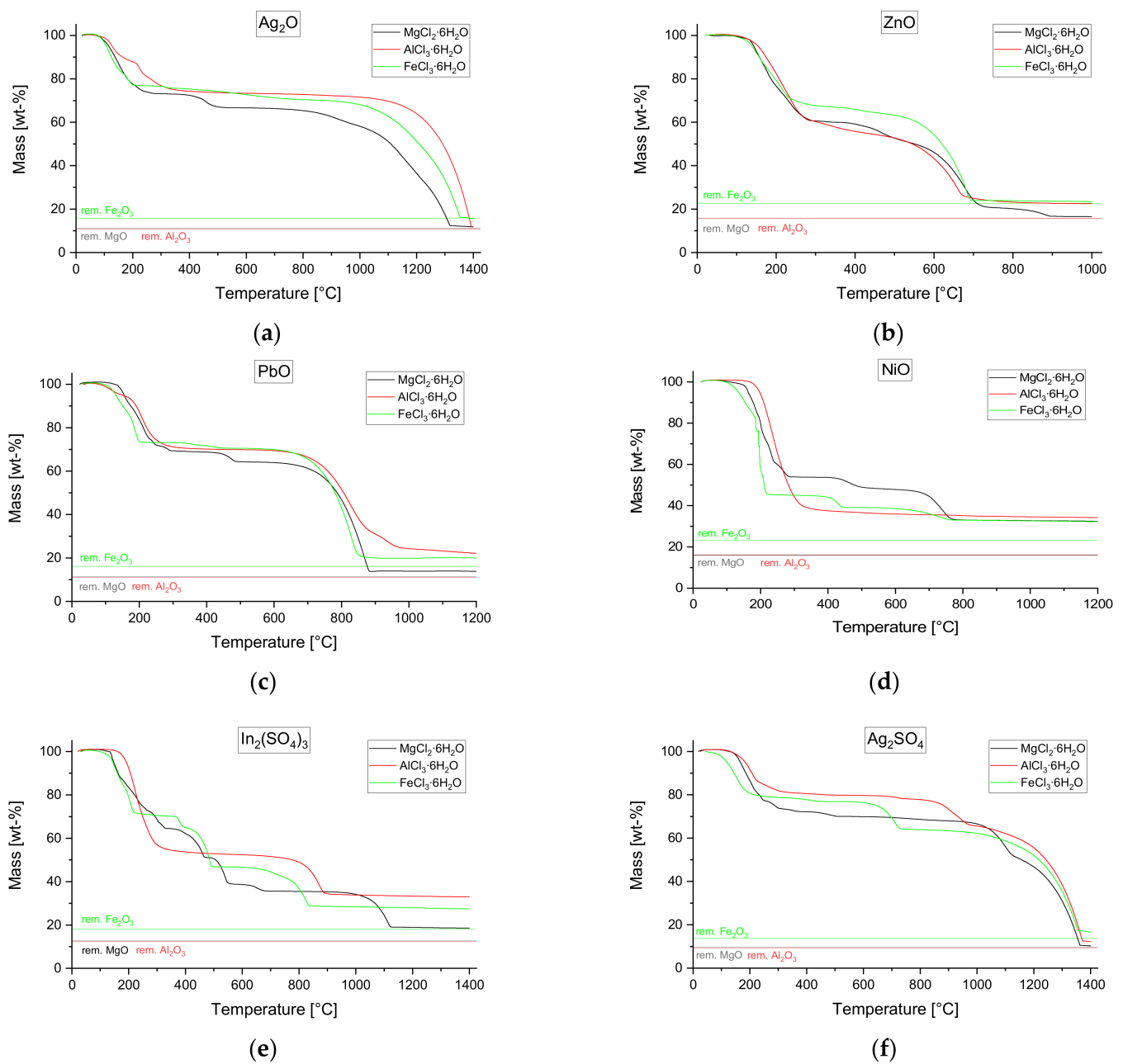


**Figure 5.** Thermogravimetric experiments with mixtures of (a)  $\text{Ag}_2\text{O}$ , (b)  $\text{ZnO}$ , (c)  $\text{PbO}$ , (d)  $\text{NiO}$ , (e)  $\text{In}_2(\text{SO}_4)_3$ , and (f)  $\text{Ag}_2\text{SO}_4$  and the three investigated chlorides  $\text{MgCl}_2 \cdot 6\text{H}_2\text{O}$ ,  $\text{AlCl}_3 \cdot 6\text{H}_2\text{O}$ , and  $\text{FeCl}_3 \cdot 6\text{H}_2\text{O}$ .

#### 4.2. Campaigns with Industrial Residues in a Muffle Furnace

The calculated valex values in Figure 6a,b show that  $\text{MgCl}_2 \cdot 6\text{H}_2\text{O}$  is the most effective chlorination agent for jarosite and calcined jarosite at the base chlorine addition factor. For all reaction systems, the yield is increased with rising temperature; when using  $\text{FeCl}_3 \cdot 6\text{H}_2\text{O}$ , it appears to be significantly increased by higher rates in the mixture (except for calcined jarosite at 900 °C).  $\text{AlCl}_3 \cdot 6\text{H}_2\text{O}$  shows the poorest outcome with very low valex values of slightly over 0.3 for the base chlorine addition. For goethite and calcined goethite (Figure 6c,d), the valex values are generally higher and less diverse with base chlorine addition; trials at 1100 °C again deliver better results compared to those at 900 °C. Yields are increased to over 90% when tripling the base addition of  $\text{FeCl}_3 \cdot 6\text{H}_2\text{O}$  for both residues. In mixtures with  $\text{MgCl}_2 \cdot 6\text{H}_2\text{O}$ , the multimetal recovery is higher when doubling the chlorine

supply and subsequently decreased (goethite) or stagnating (calcined goethite) for the three-fold addition.  $\text{AlCl}_3 \cdot 6\text{H}_2\text{O}$  again appears to be the weakest chlorination agent.

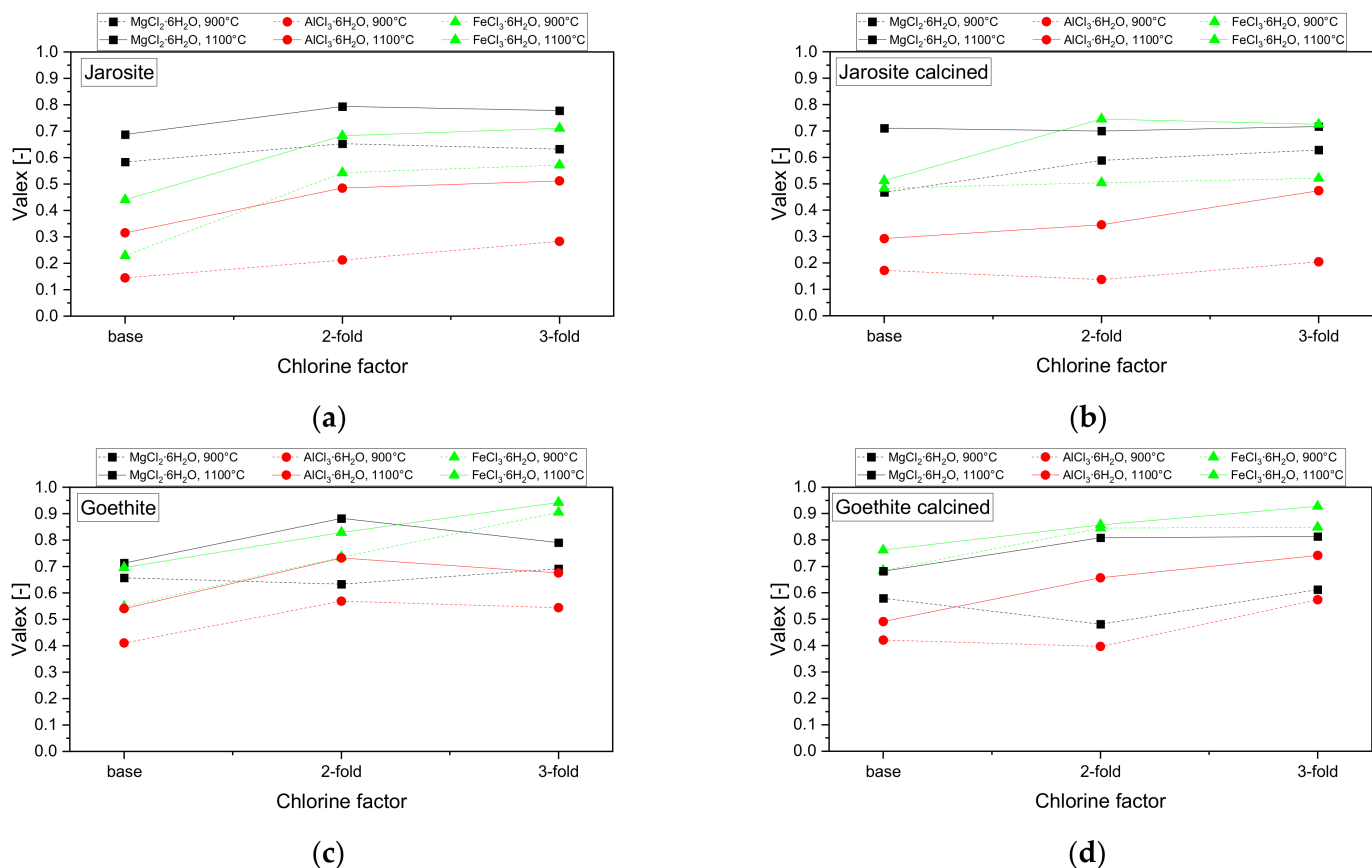


**Figure 6.** Calculated valex values of trials with precipitation residues from the zinc industry at 900 and 1100 °C. (a) Jarosite; (b) Jarosite calcined; (c) Goethite; (d) Goethite calcined.

Figure 7 shows the individual extraction rates of the elements in trials at 1100 °C. Every column is dedicated to a certain addition rate of the chloride (2Mg being the two-fold of  $\text{MgCl}_2 \cdot 6\text{H}_2\text{O}$  e.g.). Some elements such as gold and bismuth are generally very easily extracted by both  $\text{MgCl}_2 \cdot 6\text{H}_2\text{O}$  and  $\text{FeCl}_3 \cdot 6\text{H}_2\text{O}$ . Indium, zinc, and lead are preferably extracted in the presence of  $\text{MgCl}_2 \cdot 6\text{H}_2\text{O}$  from all investigated residues. Silver is hard to extract from jarosite as well as calcined jarosite, but high yields are achieved with all three chlorides from goethite. Tin is almost entirely extractable with higher additions of  $\text{FeCl}_3 \cdot 6\text{H}_2\text{O}$  from jarosite.

Nickel extraction (Figure 8a) via chlorination from original nickel jarosite is generally low with 35% being the highest yield when using the base addition of  $\text{MgCl}_2 \cdot 6\text{H}_2\text{O}$  at 1100 °C and 38% for the three-fold rate in the mixture. The valex values when using  $\text{FeCl}_3 \cdot 6\text{H}_2\text{O}$  are significantly increased by higher additions from 7% (base) to 32% at the three-fold base addition in the mixture.  $\text{AlCl}_3 \cdot 6\text{H}_2\text{O}$  reveals poor results with extraction rates of up to 18%. Extraction rates from calcined materials (Figure 8b) are lower with values of 24% and 27% for two-fold and three-fold  $\text{MgCl}_2 \cdot 6\text{H}_2\text{O}$  addition.

For all given trials, the extraction rates of iron and chlorine were furthermore calculated. Iron extraction is fluctuating whereby it is higher for trials with goethite materials. The average iron extraction over all trials is 15%. Hereby, the selective chlorination of the valuable elements is confirmed. As the chlorination of iron results in the generation of  $\text{FeCl}_3$ , which was proven to be an effective reaction agent, it is not interpreted to have a negative impact on the process performance.

In general, chlorine is entirely removed for most trials. However, for experiments with  $\text{MgCl}_2$ , it was observed that significant amounts remained in the material, especially for

trials with jarosite and calcined jarosite from the zinc industry. When treating nickel jarosite (both original and calcined), chlorine was removed entirely in all trials.

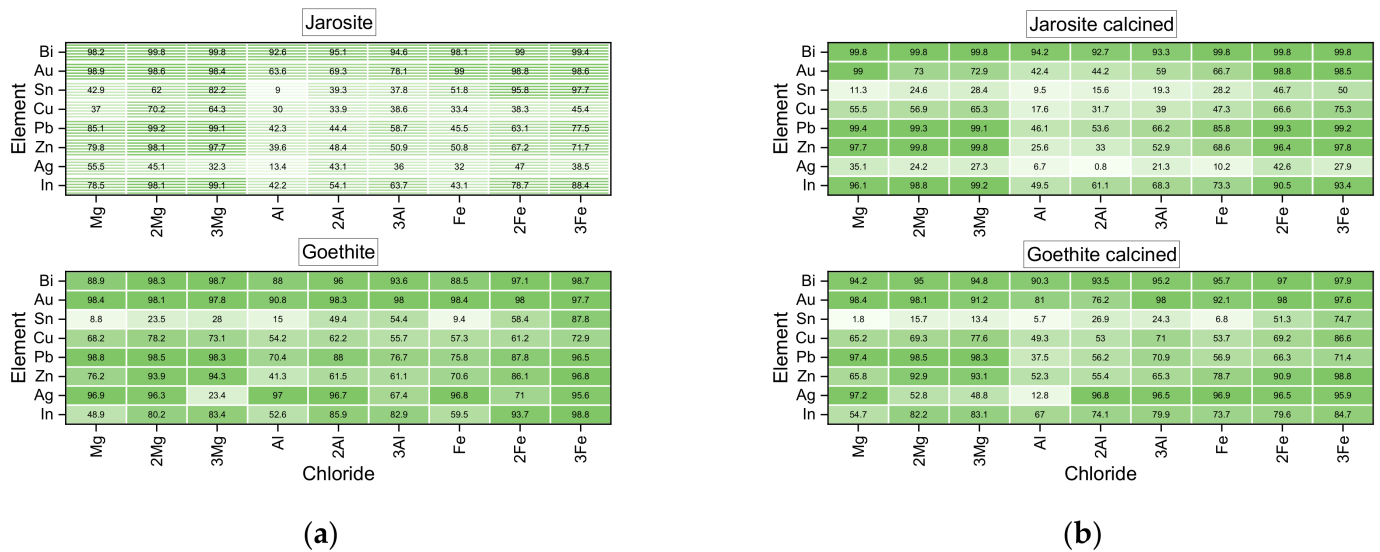


**Figure 7.** Individual extraction rates in percentage in trials at 1100 °C with (a) jarosite and goethite from the zinc industry in original as well as in (b) calcined form.

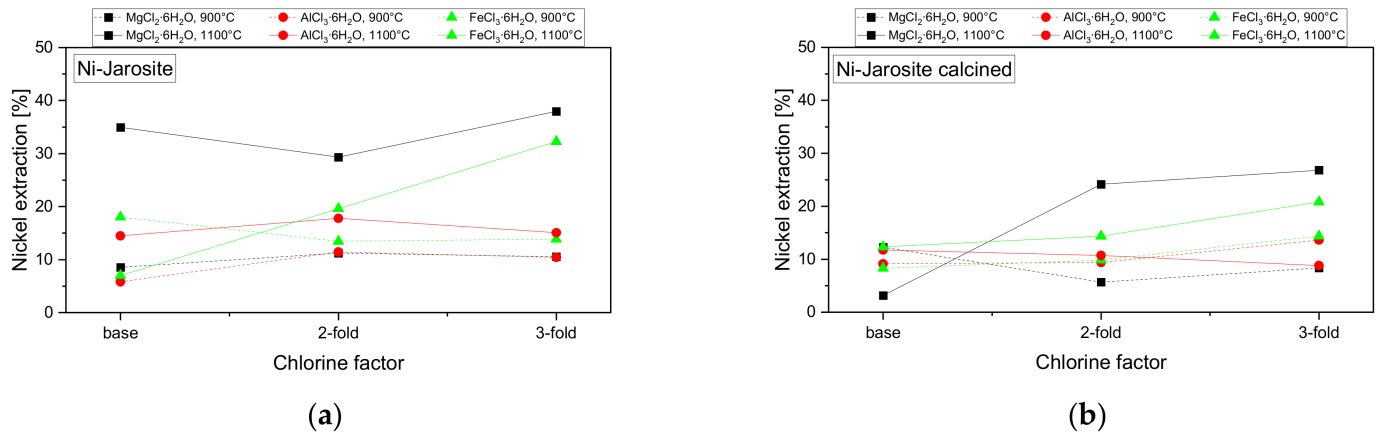


**Figure 8.** Extraction rates of nickel in trials with (a) original and (b) calcined jarosite from the nickel industry.

### 5. Discussion

To cope with the drastic climate situation and security of supply for technology metals in Europe, processes are needed that make valuable metals recoverable from residues with the lowest possible CO<sub>2</sub> emissions. In the course of thermodynamic calculations and experiments using STA, as well as in comprehensive test campaigns in a resistance-heated muffle furnace, the extraction of several valuable metals via selective chlorination was demonstrated. However, the calculations and experimental investigations carried out only provide information on the feasibility on a limited scale in a small experimental setting.

In experiments with pure substances by means of STA, the three metal chlorides MgCl<sub>2</sub>·6H<sub>2</sub>O, AlCl<sub>3</sub>·6H<sub>2</sub>O, and FeCl<sub>3</sub>·6H<sub>2</sub>O that release chlorine in the form of gaseous hydrochloric acid at increasing temperatures were identified as effective for chlorination. FeCl<sub>3</sub>·6H<sub>2</sub>O has practically a lower tendency for hydrolysis; this finding is in agreement with thermodynamic calculations. MgCl<sub>2</sub>·6H<sub>2</sub>O reacts in three hydrolysis and dehydration steps to form MgO. AlCl<sub>3</sub>·6H<sub>2</sub>O splits off the bound crystal water and chlorine in one single decomposition step. From thermodynamic calculations, it appears that the three

other chlorides NaCl, KCl, and  $\text{CaCl}_2 \cdot 6\text{H}_2\text{O}$  have lower chlorine liberation tendencies. This fact was confirmed by the practical evaluations, which showed that the chlorination of  $\text{In}_2\text{O}_3$  is not or is insufficiently possible with those three reactants.

In trials with pure valuable metal compounds, silver was proven to have a high chlorination tendency, but the extraction is aggravated by the high evaporation temperature. The chlorination and extraction of In, Zn, and Pb from oxides is feasible in mixtures with  $\text{MgCl}_2 \cdot 6\text{H}_2\text{O}$ ,  $\text{AlCl}_3 \cdot 6\text{H}_2\text{O}$ , and  $\text{FeCl}_3 \cdot 6\text{H}_2\text{O}$ , Ni shows poor chlorination behavior. In the case of sulfate compounds, chlorination is more difficult as the chlorination agents react under the formation of sulfate compounds which are subsequently decomposed. In general, lower mobility of the formed intermediate phases  $\text{SO}_2$  or  $\text{SO}_3$  can also be mentioned as a possible reason for the lower chlorination tendency. In the tests with real residual materials, a different behavior is observed when abruptly heating the mixture by charging into the hot furnace.  $\text{AlCl}_3 \cdot 6\text{H}_2\text{O}$  seems to release chlorine completely already at low temperatures due to rapid hydrolysis, where the reaction kinetics are still too low for chlorination. Only  $\text{MgCl}_2 \cdot 6\text{H}_2\text{O}$  and  $\text{FeCl}_3 \cdot 6\text{H}_2\text{O}$  could be identified as effective for chlorination from residual mixtures. Concerning a recycling process for iron precipitation residues, the addition of  $\text{FeCl}_3 \cdot 6\text{H}_2\text{O}$  is the preferred option, since no additional impurities would be introduced.

It is worth mentioning that silver can be almost entirely recovered from goethite and calcined goethite by chlorination with  $\text{MgCl}_2 \cdot 6\text{H}_2\text{O}$  and  $\text{FeCl}_3 \cdot 6\text{H}_2\text{O}$  (extraction up to 97%). Zinc, lead, gold, and bismuth are extracted in high extents from all residues of the zinc industry using the two mentioned chlorides. Nickel extraction from nickel jarosite is comparably poor, yields are even lower when the material is thermally decomposed before the experiment.  $\text{MgCl}_2 \cdot 6\text{H}_2\text{O}$  is the most effective chlorination agent followed by  $\text{FeCl}_3 \cdot 6\text{H}_2\text{O}$ . For all assessed mixtures, the yield during chlorination is significantly increased at 1100 °C compared to trials at 900 °C. Values for iron extraction are comparably low in all trials with an average yield of 15%, confirming the potential of separation of valuable elements from the excess iron matrix. Chlorine removal is effective in most trials except when  $\text{MgCl}_2 \cdot 6\text{H}_2\text{O}$  is used. The experiments served to determine which chlorides are suitable in principle and whether multimetal extraction is possible while iron remains in the residue. However, in the case of a potential large-scale implementation, many aspects have to be taken into account, which were not more closely investigated in this context. For example, the aggregate used must be heated externally or by a carbon-free burner (potentially hydrogen). Furthermore, the decomposition of the precipitation residues and the addition of the hydrated chlorides generate enormous amounts of water vapor. The large amounts of gas make it difficult to filter the chloride condensates contained in low concentrations. Furthermore, it is necessary to separate the resulting condensate fractions to recover the individual valuable metals.

## 6. Conclusions

Multimetal recovery from precipitation residues using solid chlorination agents is a promising recycling option. The best values are obtained for  $\text{MgCl}_2 \cdot 6\text{H}_2\text{O}$  and  $\text{FeCl}_3 \cdot 6\text{H}_2\text{O}$  whereby higher chloride addition results in higher yields, especially when  $\text{FeCl}_3 \cdot 6\text{H}_2\text{O}$  is used. By processing in aggregates in which the chlorine-containing atmosphere is in contact with the residual fraction for a longer time, significantly higher chlorination rates can be expected whereby the chloride additions could be significantly reduced. Furthermore, it is conceivable that the process could be carried out in the sense of combined recycling with the addition of residues that contain the chlorides in appreciable concentrations. This would result in a recycling process which, without the use of carbon as a process additive, would make it possible to recover the valuable metals contained with high economic output. Based on the investigation and positive process performance for precipitation residues as well as for the thermally decomposed residues, applicability to other residual materials is realistic.

**Supplementary Materials:** The following supporting information can be downloaded at <https://www.mdpi.com/article/10.3390/app12073590/s1>, Table S1: Experimental mixtures used in the trial campaigns at 900 °C and 1100 °C, base addition of the respective chlorides represents the approximate 2-fold of the stoichiometric demand of chlorine.

**Author Contributions:** Conceptualization, L.H. and K.W.; methodology, L.H.; software, L.H.; validation, L.H., K.W. and S.S.; writing—original draft preparation, L.H. and K.W.; writing—review and editing, L.H. and S.S.; visualization, L.H.; supervision, S.S.; project administration, L.H. and S.S.; funding acquisition, S.S. All authors have read and agreed to the published version of the manuscript.

**Funding:** This work was funded by the Austrian Federal Ministry for Digital and Economic Affairs, the National Foundation for Research, Technology and Development and the Christian Doppler Research Association.

**Institutional Review Board Statement:** Not applicable.

**Informed Consent Statement:** Not applicable.

**Data Availability Statement:** The data presented in this article are available on request from the corresponding author.

**Conflicts of Interest:** The authors declare no conflict of interest.

## References

1. Bayliss, P.; Kolitsch, U.; Nickel, E.H.; Pring, A. Alunite supergroup: Recommended nomenclature. *Mineral. Mag.* **2010**, *74*, 919–927. [[CrossRef](#)]
2. Dutrizac, J.E.; Jambor, J.L. Jarosites and Their Application in Hydrometallurgy. *Rev. Mineral. Geochem.* **2000**, *40*, 405–452. [[CrossRef](#)]
3. Sinclair, R.J. *The Extractive Metallurgy of Zinc*; Australasian Institute of Mining and Metallurgy: Carlton South, VIC, Australia, 2005; ISBN 9781613442166.
4. Calla-Choque, D.; Nava-Alonso, F.; Fuentes-Aceituno, J.C. Acid decomposition and thiourea leaching of silver from hazardous jarosite residues: Effect of some cations on the stability of the thiourea system. *J. Hazard. Mater.* **2016**, *317*, 440–448. [[CrossRef](#)] [[PubMed](#)]
5. González-Ibarra, A.A.; Nava-Alonso, F.; Uribe-Salas, A.; Castillo-Ventureño, E.N. Decomposition kinetics of industrial jarosite in alkaline media for the recovery of precious metals by cyanidation. *Can. Metall. Q.* **2016**, *55*, 448–454. [[CrossRef](#)]
6. Ju, S.; Zhang, Y.; Zhang, Y.; Xue, P.; Wang, Y. Clean hydrometallurgical route to recover zinc, silver, lead, copper, cadmium and iron from hazardous jarosite residues produced during zinc hydrometallurgy. *J. Hazard. Mater.* **2011**, *192*, 554–558. [[CrossRef](#)] [[PubMed](#)]
7. Orko, I.; Kangas, P.; Lundström, M.; Koukkari, P. Hydrometallurgical Processing of Jarosite Waste to Value-Added Products. In *3rd Symposium on Urban Mining and Circular Economy, SUM2016*; VTT Technical Research Centre of Finland Ltd.: Espoo, Finland, 2016.
8. Linsong, W.; Peng, Z.; Yu, F.; Sujun, L.; Yue, Y.; Li, W.; Wei, S. Recovery of metals from jarosite of hydrometallurgical nickel production by thermal treatment and leaching. *Hydrometallurgy* **2020**, *198*, 105493. [[CrossRef](#)]
9. Hoeber, L.; Steinlechner, S. A comprehensive review of processing strategies for iron precipitation residues from zinc hydrometallurgy. *Clean. Eng. Technol.* **2021**, *4*, 100214. [[CrossRef](#)]
10. Asokan, P.; Saxena, M.; Asolekar, S.R. Hazardous jarosite use in developing non-hazardous product for engineering application. *J. Hazard. Mater.* **2006**, *137*, 1589–1599. [[CrossRef](#)]
11. Asokan, P.; Saxena, M.; Asolekar, S.R. Recycling hazardous jarosite waste using coal combustion residues. *Mater. Charact.* **2010**, *61*, 1342–1355. [[CrossRef](#)]
12. Pappu, A.; Thakur, V.K.; Patidar, R.; Asolekar, S.R.; Saxena, M. Recycling marble wastes and Jarosite wastes into sustainable hybrid composite materials and validation through Response Surface Methodology. *J. Clean. Prod.* **2019**, *240*, 118249. [[CrossRef](#)]
13. Mymrin, V.; Vazquez Vaamonde, A. New construction materials from Spanish jarosite processing wastes. *Miner. Eng.* **1999**, *12*, 1399–1402. [[CrossRef](#)]
14. Mymrin, V.A.; Ponte, H.A.; Impinnisi, P.R. Potential application of acid jarosite wastes as the main component of construction materials. *Constr. Build. Mater.* **2005**, *19*, 141–146. [[CrossRef](#)]
15. Mehra, P.; Gupta, R.C.; Thomas, B.S. Properties of concrete containing jarosite as a partial substitute for fine aggregate. *J. Clean. Prod.* **2016**, *120*, 241–248. [[CrossRef](#)]
16. Katsioti, M.; Boura, P.; Agatzini, S.; Tsakiridis, P.E.; Oustadakis, P. Use of jarosite/alunite precipitate as a substitute for gypsum in Portland cement. *Cem. Concr. Compos.* **2005**, *27*, 3–9. [[CrossRef](#)]

17. Winters, J.; Vos, L.; Canoo, C. Goethite: From Residue to Secondary Building Material-Union Minière's Graveliet<sup>®</sup> Process. In Proceedings of the Lead-Zinc 2000 Symposium which was part of the TMS Fall Extraction & Process Metallurgy Meeting, Pittsburgh, PA, USA, 22–25 October 2000; Dutrizac, J.E., Ed.; TMS: Warrendale, PA, USA, 2000; pp. 903–916; ISBN 9781118805558.
18. Castro, L.; Blázquez, M.L.; González, F.; Muñoz, J.A.; Ballester, A. Reductive leaching of jarosites by *Aeromonas hydrophila*. *Miner. Eng.* **2016**, *95*, 21–28. [[CrossRef](#)]
19. Castro, L.; García-Balboa, C.; González, F.; Ballester, A.; Blázquez, M.L.; Muñoz, J.A. Effectiveness of anaerobic iron bio-reduction of jarosite and the influence of humic substances. *Hydrometallurgy* **2013**, *131–132*, 29–33. [[CrossRef](#)]
20. Mäkinen, J.; Salo, M.; Hassinen, H.; Kinnunen, P. Comparison of Reductive and Oxidative Bioleaching of Jarosite for Valuable Metals Recovery. *Solid State Phenom.* **2017**, *262*, 24–27. [[CrossRef](#)]
21. Boháček, J.; Šubrt, J.; Hanslík, T.; Tláskal, J. Preparing particulate magnetites with pigment properties from suspensions of basic iron(III) sulphates with the structure of jarosite. *J. Mater. Sci.* **1993**, *28*, 2827–2832. [[CrossRef](#)]
22. Dutrizac, J.E. Converting jarosite residues into compact hematite products. *JOM* **1990**, *42*, 36–39. [[CrossRef](#)]
23. Röpenack, A.; Böhmer, W.; Rieger, H. Verfahren zur Aufarbeitung von Jarosit-Haltigen Rückständen. European Patent Application 90202618.6, 2 October 1990.
24. Cruells, M.; Roca, A.; Patiño, F.; Salinas, E.; Rivera, I. Cyanidation kinetics of argentian jarosite in alkaline media. *Hydrometallurgy* **2000**, *55*, 153–163. [[CrossRef](#)]
25. Patiño, F.; Cruells, M.; Roca, A.; Salinas, E.; Pérez, M. Kinetics of alkaline decomposition and cyanidation of argentian ammonium jarosite in lime medium. *Hydrometallurgy* **2003**, *70*, 153–161. [[CrossRef](#)]
26. Patiño, F.; Salinas, E.; Cruells, M.; Roca, A. Alkaline decomposition–cyanidation kinetics of argentian natrojarosite. *Hydrometallurgy* **1998**, *49*, 323–336. [[CrossRef](#)]
27. Patiño, F.; Viñals, J.; Roca, A.; Núñez, C. Alkaline decomposition–cyanidation kinetics of argentian plumbojarosite. *Hydrometallurgy* **1994**, *34*, 279–291. [[CrossRef](#)]
28. Hage, J.L.T.; Schuiling, R.D.; Vriend, S.P. Production of Magnetite from Sodiumjarosite under Reducing Hydrothermal Conditions. The Reduction of Fe III to Fe II with Cellulose. *Can. Metall. Q.* **1999**, *38*, 267–276. [[CrossRef](#)]
29. Han, H.; Sun, W.; Hu, Y.; Jia, B.; Tang, H. Anglesite and silver recovery from jarosite residues through roasting and sulfidation–flotation in zinc hydrometallurgy. *J. Hazard. Mater.* **2014**, *278*, 49–54. [[CrossRef](#)]
30. Riley, A.L.; Pepper, S.E.; Canner, A.J.; Brown, S.F.; Ogden, M.D. Metal recovery from jarosite waste—A resin screening study. *Sep. Sci. Technol.* **2018**, *53*, 22–35. [[CrossRef](#)]
31. Rodríguez, N.; Machiels, L.; Onghena, B.; Spooren, J.; Binnemans, K. Selective recovery of zinc from goethite residue in the zinc industry using deep-eutectic solvents. *RSC Adv.* **2020**, *10*, 7328–7335. [[CrossRef](#)]
32. Creedy, S.; Glinin, A.; Matuszewicz, R.; Hughes, S.; Reuter, M. Ausmelt Technology for Treating Zinc Residues. *World Metall. Erzmetall* **2013**, *66*, 230.
33. Salminen, J.; Nyberg, J.; Imris, M.; Heegaard, B.M. Smelting Jarosite and Sulphur Residue in a Plasma Furnace. In *PBZN 2020: The 9th International Symposium on Lead and Zinc Processing*; Siegmund, A., Alam, S., Grogan, J., Kerney, U., Shibata, E., Eds.; Springer Nature: Berlin/Heidelberg, Germany, 2020; pp. 391–403; ISBN 978-3-030-37069-5.
34. Mombelli, D.; Mapelli, C.; Barella, S.; Gruttadauria, A.; Spada, E. Jarosite wastes reduction through blast furnace sludges for cast iron production. *J. Environ. Chem. Eng.* **2019**, *7*, 102966. [[CrossRef](#)]
35. Piga, L.; Stoppa, L.; Massidda, R. Recycling of industrial goethite wastes by thermal treatment. *Resour. Conserv. Recycl.* **1995**, *14*, 11–20. [[CrossRef](#)]
36. Pelino, M.; Cantalini, C.; Abbruzzese, C.; Plescia, P. Treatment and recycling of goethite waste arising from the hydrometallurgy of zinc. *Hydrometallurgy* **1996**, *40*, 25–35. [[CrossRef](#)]
37. Pelino, M.; Cantalini, C.; Boattini, P.P.; Abbruzzese, C.; Rincon, J.; Garcia Hernandez, J.E. Glass-ceramic materials obtained by recycling goethite industrial wastes. *Resour. Conserv. Recycl.* **1994**, *10*, 171–176. [[CrossRef](#)]
38. Steinlechner, S.; Antrekowitsch, J. Thermodynamic Considerations for a Pyrometallurgical Extraction of Indium and Silver from a Jarosite Residue. *Metals* **2018**, *8*, 335. [[CrossRef](#)]
39. Wegscheider, S.; Steinlechner, S.; Leuchtenmüller, M. Innovative Concept for the Recovery of Silver and Indium by a Combined Treatment of Jarosite and Electric Arc Furnace Dust. *JOM* **2017**, *69*, 388–394. [[CrossRef](#)]
40. Wang, Y.; Yang, H.; Zhang, G.; Kang, J.; Wang, C. Comprehensive recovery and recycle of jarosite residues from zinc hydrometallurgy. *Chem. Eng. J. Adv.* **2020**, *3*, 100023. [[CrossRef](#)]
41. Guan, J.; Wang, S.; Ren, H.; Guo, Y.; Yuan, H.; Yan, X.; Guo, J.; Gu, W.; Su, R.; Liang, B.; et al. Indium recovery from waste liquid crystal displays by polyvinyl chloride waste. *RSC Adv.* **2015**, *5*, 102836–102843. [[CrossRef](#)]
42. Park, K.-S.; Sato, W.; Grause, G.; Kameda, T.; Yoshioka, T. Recovery of indium from In<sub>2</sub>O<sub>3</sub> and liquid crystal display powder via a chloride volatilization process using polyvinyl chloride. *Thermochim. Acta* **2009**, *493*, 105–108. [[CrossRef](#)]
43. Takahashi, K.; Sasaki, A.; Dodbiba, G.; Sadaki, J.; Sato, N.; Fujita, T. Recovering Indium from the Liquid Crystal Display of Discarded Cellular Phones by Means of Chloride-Induced Vaporization at Relatively Low Temperature. *Metall. Mater. Trans. A* **2009**, *40*, 891–900. [[CrossRef](#)]
44. Gustafsson, A.M.; Steenari, B.-M.; Ekberg, C. Recycling of CIGS solar cell waste materials—separation of copper, indium and gallium by high-temperature chlorination reaction with ammonium chloride. *Sep. Sci. Technol.* **2015**, *38*, 2415–2425. [[CrossRef](#)]

45. Li, H.; Ma, A.; Srinivasakannan, C.; Zhang, L.; Li, S.; Yin, S. Investigation on the recovery of gold and silver from cyanide tailings using chlorination roasting process. *J. Alloys Compd.* **2018**, *763*, 241–249. [[CrossRef](#)]
46. Qin, H.; Guo, X.; Tian, Q.; Zhang, L. Pyrite enhanced chlorination roasting and its efficacy in gold and silver recovery from gold tailing. *Sep. Purif. Technol.* **2020**, *250*, 117168. [[CrossRef](#)]
47. Jaafar, I.; Griffiths, A.J.; Hopkins, A.C.; Steer, J.M.; Griffiths, M.H.; Sapsford, D.J. An evaluation of chlorination for the removal of zinc from steelmaking dusts. *Miner. Eng.* **2011**, *24*, 1028–1030. [[CrossRef](#)]
48. Kurashima, K.; Matsuda, K.; Kumagai, S.; Kameda, T.; Saito, Y.; Yoshioka, T. A combined kinetic and thermodynamic approach for interpreting the complex interactions during chloride volatilization of heavy metals in municipal solid waste fly ash. *Waste Manag.* **2019**, *87*, 204–217. [[CrossRef](#)]
49. Wang, S.-J.; He, P.-J.; Lu, W.-T.; Shao, L.-M.; Zhang, H. Comparison of Pb, Cd, Zn, and Cu chlorination during pyrolysis and incineration. *Fuel* **2017**, *194*, 257–265. [[CrossRef](#)]
50. Nowak, B.; Frías Rocha, S.; Aschenbrenner, P.; Rechberger, H.; Winter, F. Heavy metal removal from MSW fly ash by means of chlorination and thermal treatment: Influence of the chloride type. *Chem. Eng. J.* **2012**, *179*, 178–185. [[CrossRef](#)]
51. Yu, J.; Sun, L.; Ma, C.; Qiao, Y.; Xiang, J.; Hu, S.; Yao, H. Mechanism on heavy metals vaporization from municipal solid waste fly ash by  $MgCl_2 \cdot 6H_2O$ . *Waste Manag.* **2016**, *49*, 124–130. [[CrossRef](#)] [[PubMed](#)]
52. Silver Price. Available online: <https://www.goldpreis.de/silberpreis/> (accessed on 29 December 2021).
53. Gold Price. Available online: <https://www.goldpreis.de/> (accessed on 29 December 2021).
54. Bismuth Price. Available online: <https://price.metal.com/Bismuth-Selenium-Tellurium> (accessed on 29 December 2021).
55. Copper Price. Available online: <https://www.finanzen.at/rohstoffe/kupferpreis> (accessed on 29 December 2021).
56. Indium Price. Available online: <http://www.indium-preis.de/> (accessed on 29 December 2021).
57. Lead Price. Available online: <https://www.finanzen.at/rohstoffe/bleipreis> (accessed on 29 December 2021).
58. Tin Price. Available online: <https://www.finanzen.at/rohstoffe/zinnpreis> (accessed on 29 December 2021).
59. Zinc Price. Available online: <https://www.finanzen.at/rohstoffe/zinkpreis> (accessed on 29 December 2021).
60. Zboril, R.; Mashlan, M.; Papaefthymiou, V.; Hadjipanayis, G. Thermal decomposition of  $Fe_2(SO_4)_3$ : Demonstration of  $Fe_2O_3$  polymorphism. *J. Radioanal. Nucl. Chem.* **2003**, *255*, 413–417. [[CrossRef](#)]
61. Pelovski, Y.; Pietkova, W.; Gruncharov, I.; Pacewska, B.; Pysiak, J. The thermal decomposition of aluminum sulfate in different gas phase environments. *Thermochim. Acta* **1992**, *205*, 219–224. [[CrossRef](#)]
62. Scheidema, M.N.; Taskinen, P. Decomposition Thermodynamics of Magnesium Sulfate. *Ind. Eng. Chem. Res.* **2011**, *50*, 9550–9556. [[CrossRef](#)]